Journal of Computational Physics **160,** 500–521 (2000)
doi:10.1006/jcph.2000.6468, available online at http://www.idealibrary.com on IDEAL®

High-Order Scheme for a Nonlinear Maxwell System Modelling Kerr Effect

Armel de La Bourdonnaye

Ecole Nationale des Ponts et Chaussees-INRIA, CERMICS, BP93, 06902 Sophia Antipolis Cedex, France

Received May 24, 1999; revised December 23, 1999

This paper is devoted to the derivation of an efficient numerical scheme for the Kerr–Maxwell system. We begin by studying the 1-D Riemann problem. We obtain a result of existence and uniqueness for large data. Then we develop a high-order Roe solver and exhibit solutions in 1-D and 2-D simulations.

Key Words: Maxwell system; Kerr effect; quasilinear system; hyperbolicity; Godunov solver; Roe solver; filamentation.

1. INTRODUCTION

The domain of nonlinear optics is a very active one and involves activities of physical modelling, experimentations, mathematical analysis, and numerical simulation (see [1, 7], for instance). Some interesting applications can be found in the domains of lasers, propagation through optic fibers and design of optic devices, and interactions between lasers and plasmas, for instance. The basic model is the Maxwell–Bloch model, which is based on the interaction between the electromagnetic field and atoms with one rest state and one excited state. Nonetheless some phenomenological models are proposed in the literature. One frequently used is the Kerr model

$$\begin{aligned} \partial_t B + \mathrm{curl} E &= 0 \\ \partial_t D - \mathrm{curl} H &= 0 \end{aligned} \tag{1}$$

with the constitutive laws

$$\begin{aligned} B &= \mu_0 H \\ D &= \epsilon_0 E + P_{\mathrm{L}} + P_{\mathrm{NL}} \\ P_{\mathrm{NL}} &= \alpha |E|^2 E \\ \partial_{t^2}^2 P_{\mathrm{L}} + (1/T)\partial_t P_{\mathrm{L}} + \Omega^2 P_{\mathrm{L}} &= \gamma E. \end{aligned} \tag{2}$$

0021-9991/00 $35.00

Here, and in the rest of the paper also, B, E, H, and D denote, respectively, the magnetic field, the electric field, the magnetic induction, and the electric displacement. P_{L} is the linear polarisation and P_{NL} is the nonlinear polarisation. This is the model we will study in what follows. More precisely, and for reasons of simplicity, since we want to focus on the nonlinear effects, we will also assume that $P_{\mathrm{L}} = 0$. The main classical way to deal with these models is to perform a two-time-scale analysis. The fast time scale is tied to the frequency of the electromagnetic wave, and the slow one is tied to the variations of the envelope of the wave. This generally leads to nonlinear Schroedinger equations. A lot of work has been done to give a precise mathematical meaning to these formal asymptotic exansions. Furthermore, in the case of Maxwell–Bloch system, a result of existence and uniqueness has been obtained (see [5]). As far as we know there is no similar result for the Kerr model. In the domain of numerical methods, we can mention the work of Donat [4], which presents a 1-D finite volume method based on a Roe solver and a 2-D finite element method, and the work of Taflove [16] around a finite difference method. The purpose of this paper is to develop and present an efficient numerical scheme to simulate this phenomenon even with unstructured meshes. Section 2 will present some mathematical results, mostly from the viewpoint of hyperbolic systems. Section 3 will present our numerical scheme, which is based on the Roe solver extended to third order by a MUSCL technique and on a three-step Runge–Kutta scheme. We will end up with some numerical results in one and two spatial dimensions.

2. THE MATHEMATICAL STUDY OF THE SYSTEM

2.1. Hyperbolicity of the System

We consider the following model. Let $\mathcal{L}(E, B)$ be a Lagrangian. We suppose that

$$\mathcal{L}(E, B) = \mathcal{E}\left(\frac{|E|^2}{2}\right) - \frac{|B|^2}{2}$$

is strictly convex with respect to E (we assume that there exists a positive definite matrix P so that the second derivative of $\mathcal{E}(|E|^2/2)$ is greater then P, for all E). Then we define the electric displacement D by

$$D = \frac{\partial \mathcal{L}}{\partial E} = \mathcal{E}' E.$$

So the Hamiltonian $\mathcal{H}(D, B) = D \cdot E - \mathcal{L}(E, B)$ is a convex energy since it is a Moreau dual function of $\mathcal{L}$ (see [14, p. 46] for instance). This amounts to

$$\mathcal{E}'\left(\frac{X^2}{2}\right) \geq 0; \qquad \mathcal{E}'\left(\frac{X^2}{2}\right) + X^2 \mathcal{E}''\left(\frac{X^2}{2}\right) \geq 0 \quad \text{for } X > 0.$$

The convexity of the energy implies that the function $D(E)$ is invertible. We also restrict ourselves to super-quadratic energies.

DEFINITION 2.1. The convex function $f(X)$ is said to be super-quadratic if, by definition,

$$\forall X, \qquad Y(|X|^2 - |Y|^2) \cdot \left(\frac{\partial_X f(X) + \partial_X f(Y)}{2} \cdot (X - Y) - (f(X) - f(Y))\right) \geq 0.$$

This implies that

$$\partial^3_{XXX} f(X)(\delta,\delta,\delta) \qquad \text{has the same sign as } X\cdot\delta.$$

We remark that with this definition, every function of the type $|X|^{2+\alpha}$, $\alpha>0$ is super-quadratic. This leads to $\mathcal{E}''(X^2/2)>0$.

So the Maxwell system we consider is

$$\begin{aligned}\partial_t D - \operatorname{curl} B &= 0\\ \partial_t B + \operatorname{curl} E(D) &= 0.\end{aligned} \tag{3}$$

We may rewrite this in a nonconservative form:

$$\begin{cases}\partial_t D - \operatorname{curl} B = 0\\ \partial_t B + \left(\frac{\partial D}{\partial E}\right)^{-1}\operatorname{curl} D = 0\end{cases} \tag{4}$$

Here, we introduce

$$J = \frac{\partial D}{\partial E} = \frac{\partial^2 \mathcal{H}}{\partial E^2} = \mathcal{E}'\cdot Id + \mathcal{E}''\cdot E\otimes E \tag{5}$$

LEMMA 2.1. *$\mathcal{E}'+\mathcal{E}''|E|^2$ is an eigenvalue of multiplicity 1 of J which is associated to the eigenvector E. $\mathcal{E}'$ is an eigenvalue of multiplicity 2 of J which is associated to the eigenspace which is orthogonal to E.*

Proof. The proof is left to the reader. ■

LEMMA 2.2. *The system* (4) *is a quasilinear hyperbolic and symmetrisable system.*

Proof. Indeed, the symbol of the system is

$$K = \left(\begin{array}{c|c} I_3 & 0_3\\ \hline 0_3 & J^{-1}\end{array}\right)\cdot\left(\begin{array}{c|c} 0_3 & i\xi\wedge\\ \hline -i\xi\wedge & 0_3\end{array}\right), \tag{6}$$

where ξ is the symbol of the space derivation and $i\xi\wedge$ stands for the matrix of the operator

$$E\in\mathbb{R}^3 :\mapsto i\xi\wedge E.$$

First, we observe that $\binom{\xi}{0}$ and $\binom{0}{\xi}$ are eigenvectors of K for 0 as an eigenvalue.

Second, we observe that $\xi\wedge E$ is an $\mathcal{E}'$-eigenvector of J. Thus,

$$\begin{pmatrix}\xi\wedge E\\ \frac{\pm}{|\xi|\sqrt{\mathcal{E}'}}\xi\wedge(\xi\wedge E)\end{pmatrix}$$

is an eigenvector of K associated to the eigenvalue $\lambda_1^{\pm}=\mp i|\xi|/\sqrt{\mathcal{E}'}$.

Finally, we have to find the last pair of eigenvectors. Let us denote it by $\binom{V1}{V2}$ and the eigenvalue by λ. We have

$$i\xi\wedge V2 = \lambda V1 \tag{7}$$

$$J^{-1}(-i\xi\wedge V1) = \lambda V2. \tag{8}$$

Thus,

$$J(V2) = \frac{-|\xi|^2}{\lambda^2} V2^{\perp}, \tag{9}$$

where $V^{\perp}$ denotes $V - (1/|\xi|^2)(V \cdot \xi)\xi$. It is easy to check that we can look for $V2$ in the space spanned by $(\xi, E^{\top})$. This is due to the special shape of J. Let

$$W = \left(JE^{\top}, \frac{\xi}{|\xi|}\right)\frac{\xi}{|\xi|} - \left(J\frac{\xi}{|\xi|}, \frac{\xi}{|\xi|}\right)E^{\top}. \tag{10}$$

We have $(JW, \xi) = 0$ and $(JW, \xi \wedge E) = 0$. Furthermore,

$$(JW, E^{\top}) = \frac{\left(J\frac{E^{\top}}{|E^{\top}|}, \frac{\xi}{|\xi|}\right)^2 - \left(J\frac{\xi}{|\xi|}, \frac{\xi}{|\xi|}\right)\left(J\frac{E^{\top}}{|E^{\top}|}, \frac{E^{\top}}{|E^{\top}|}\right)}{-\left(J\frac{\xi}{|\xi|}, \frac{\xi}{|\xi|}\right)} \cdot (W^{\top}, E^{\top}). \tag{11}$$

Thus we can choose $V2 = W$ and we have

$$\lambda^2 = \frac{-|\xi|^2\left(J\frac{\xi}{|\xi|}, \frac{\xi}{|\xi|}\right)}{\left(J\frac{E^{\top}}{|E^{\top}|}, \frac{\xi}{|\xi|}\right)^2 - \left(J\frac{\xi}{|\xi|}, \frac{\xi}{|\xi|}\right)\left(J\frac{E^{\top}}{|E^{\top}|}, \frac{E^{\top}}{|E^{\top}|}\right)}. \tag{12}$$

If we use formula (5), we obtain

$$\lambda^2 = \frac{-|\xi|^2}{\mathcal{E}'}\frac{\left(J\frac{\xi}{|\xi|}, \frac{\xi}{|\xi|}\right)}{\left(J\frac{E}{|E|}, \frac{E}{|E|}\right)}. \tag{13}$$

We denote

$$\lambda_2^{\pm} = \frac{\pm i|\xi|}{\sqrt{\mathcal{E}'}}\sqrt{\frac{\left(J\frac{\xi}{|\xi|}, \frac{\xi}{|\xi|}\right)}{\left(J\frac{E}{|E|}, \frac{E}{|E|}\right)}} \tag{14}$$

and we finally obtain that

$$\begin{pmatrix} \frac{i\xi}{\lambda_2^{\pm}} \wedge W \\ W \end{pmatrix}$$

is en eigenvector for the eigenvalue $\lambda_2^{\pm}$. The fact that all the six eigenvalues are pure imaginary numbers shows that the system is hyperbolic. If we let

$$R = \left(\begin{array}{c|c} I_3 & 0_3 \\ \hline 0_3 & J \end{array}\right), \tag{15}$$

we obtain that $RK + (RK)^{\star} = 0$, so the system is symmetrisable. ■

Using these results and [17, Thm. 5.6, p. 89], we can derive existence and uniqueness results for small time and regular enough initial data in $\mathbb{R}^3$. In [13], one can also find results for small and regular initial data in long time range.

2.2. The 1-D Case

Since the system is hyperbolic we aim at using classical finite volume methods. They are based on the computation of 1-D problems in the directions which are normal to the interfaces between two adjacent cells. For this reason, we will study the 1-D Kerr–Maxwell system. So we consider that we have 3-D fields but the propagation occurs only in the x-direction. So $\partial_t D_x = \partial_t B_x = 0$. Also,

$$\begin{aligned} \partial_t(D_y) + \partial_x(B_z) &= 0 \\ \partial_t(D_z) + \partial_x(-B_y) &= 0 \\ \partial_t(B_z) + \partial_x(E_y) &= 0 \\ \partial_t(-B_y) + \partial_x(E_z) &= 0. \end{aligned} \tag{16}$$

We denote (E_y, E_z) by $\tilde{E}$, (D_y, D_z) by $\tilde{B}$ and $(B_z, -B_y)$ by $\tilde{B}$. Thus the nonconservative form is

$$\partial_t W + \left(\begin{array}{c|c} 0_2 & I_2 \\ \hline \tilde{J}^{-1} & 0_2 \end{array}\right) \partial_x W = 0, \tag{17}$$

where $\tilde{J}^{-1}$ is the restriction of the matrix J^{-1} to D_y, D_z. Since

$$J = \mathcal{E}' \cdot Id + \mathcal{E}'' \cdot E \otimes E, \tag{18}$$

$$J^{-1} = \frac{Id}{\mathcal{E}'} - \frac{\mathcal{E}'' E \otimes E}{\mathcal{E}'(\mathcal{E}' + \mathcal{E}''|E|^2)}, \tag{19}$$

and

$$\tilde{J}^{-1} = \frac{Id}{\mathcal{E}'} - \frac{\mathcal{E}''\tilde{E} \otimes \tilde{E}}{\mathcal{E}'(\mathcal{E}' + \mathcal{E}''|E|^2)}. \tag{20}$$

Its eigenvalues are $1/\mathcal{E}'$ and $1/(\mathcal{E}' + \mathcal{E}''|E|^2)$. They are associated to the eigenvectors $\tilde{E}_\perp = (-E_z, E_y)$ and $\tilde{E}$. So we have

LEMMA 2.3. *The eigenvalues of the* 1*-D Kerr–Maxwell system are*

$$\begin{aligned} \lambda_1^{\pm} &= \frac{\pm 1}{\sqrt{\mathcal{E}'}} \\ \lambda_2^{\pm} &= \frac{\pm 1}{\sqrt{\mathcal{E}' + \mathcal{E}''|E|^2}}, \end{aligned} \tag{21}$$

corresponding to the eigenvectors

$$\begin{aligned} W_1^{\pm} &= \left(\tilde{E}_\perp, \frac{\pm\tilde{E}_\perp}{\sqrt{\mathcal{E}'}}\right) \\ W_2^{\pm} &= \left(\tilde{E}, \frac{\pm\tilde{E}}{\sqrt{\mathcal{E}' + \mathcal{E}''|E|^2}}\right). \end{aligned} \tag{22}$$

We leave this simple proof to the reader. It also easy to see that the first pair of fields is linearly degenerate. Furthermore, one can also check that the second pair of fields is neither linearly degenerate (except when the system is linear), nor genuinely nonlinear, generally speaking. We finally remark that the characteristic speed of the 1-waves is greater than the speed of the 2-waves, thanks to the super-quadratic assumption. Now we can look for the Riemann invariants. There are three of them for each eigenvalue; they are denoted by $R^{\pm}_{1\text{ or }2,j}$, with $j = 1, \dots, 3$.

LEMMA 2.4. *We have*

$$\begin{aligned} R^{\pm}_{1,1} &= |\tilde{E}|^2 \\ \begin{pmatrix} R^{\pm}_{1,2} \\ R^{\pm}_{1,3} \end{pmatrix} &= \sqrt{\mathcal{E}'}\tilde{E} \mp \tilde{B} \\ R^{\pm}_{2,1} &= \tilde{E}/|\tilde{E}| \\ \begin{pmatrix} R^{\pm}_{2,2} \\ R^{\pm}_{2,3} \end{pmatrix} &= G(|\tilde{E}|)\frac{\tilde{E}}{|\tilde{E}|} \mp \tilde{B} \end{aligned} \tag{23}$$

with

$$\frac{dG(|\tilde{E}|)}{d|\tilde{E}|} = \sqrt{\mathcal{E}' + \mathcal{E}''|E|^2}.$$

Here, one has to take care of the fact that the argument of $\mathcal{E}$ and its derivatives is

$$\frac{|E|^2}{2} = \frac{|E_x|^2 + |\tilde{E}|^2}{2}.$$

Proof. First, notice that $\partial_w = (\partial_D, \partial_B) = (\tilde{J}^{-1}\partial_E, \partial_B)$.
Let us begin with the first pair of eigenvalues:

$$\partial_W R^{\pm}_{1,1} \cdot W^{\pm}_1 = (2\tilde{J}^{-1}\tilde{E}, 0) \cdot \left(\tilde{E_\perp}, \frac{\pm\tilde{E}_\perp}{\sqrt{\mathcal{E}'}} \right) = 0.$$

Similarly,

$$\partial_W \begin{pmatrix} R^{\pm}_{1,2} \\ R^{\pm}_{1,3} \end{pmatrix} \cdot W^{\pm}_1 = \begin{pmatrix} (\sqrt{\mathcal{E}'})'\tilde{J}^{-1}\tilde{E} \otimes \tilde{E} + \sqrt{\mathcal{E}'}\tilde{J}^{-1} \\ \mp I \end{pmatrix} \begin{pmatrix} \tilde{E}_\perp \\ \frac{\pm\tilde{E}_\perp}{\sqrt{\mathcal{E}'}} \end{pmatrix} \tag{24}$$

$$= \frac{\tilde{E}_\perp}{\sqrt{\mathcal{E}'}} - \frac{\tilde{E}_\perp}{\sqrt{\mathcal{E}'}} \tag{25}$$

$$= 0. \tag{26}$$

In the same way, for the second pair of eigenvalues,

$$\partial_W R^{\pm}_{2,1} \cdot W^{\pm}_2 = \left(\frac{\tilde{J}^{-1}}{|\tilde{E}|} - \frac{(\tilde{J}^{-1}\tilde{E}) \otimes \tilde{E}}{|\tilde{E}|^3} \right) \cdot \tilde{E} = 0$$

and

$$\partial_W \begin{pmatrix} R^{\pm}_{2,2} \\ R^{\pm}_{2,3} \end{pmatrix} \cdot W^{\pm}_2 \tag{27}$$

$$= \begin{pmatrix} \tilde{J}^{-1}\left(G'(|\tilde{E}|)\frac{\tilde{E}\otimes\tilde{E}}{|\tilde{E}|^2} + \frac{G|\tilde{E}|^2 - G\tilde{E}\otimes\tilde{E}}{|\tilde{E}|^2}\right) \\ \mp I \end{pmatrix} \begin{pmatrix} \tilde{E} \\ \frac{\pm\tilde{E}}{\sqrt{\mathcal{E}' + \mathcal{E}''|\tilde{E}|^2}} \end{pmatrix} \tag{28}$$

$$= \frac{G'\tilde{E}}{\mathcal{E}' + \mathcal{E}''|\tilde{E}|^2} - \frac{1}{\sqrt{\mathcal{E}' + \mathcal{E}''|\tilde{E}|^2}}\tilde{E} \tag{29}$$

$$= 0. \tag{30}$$

This ends the proof. ■

At this stage, we make some remarks.

Remark. If we suppose that the electrical energy $\mathcal{E}$ is smooth in the neighborhood of 0, then the only case where one can have a genuinely nonlinear field is when $\mathcal{E} = \alpha|E|^2$ but this corresponds to the linearly degenerate case.

Remark. The special forms of $R^{\pm}_{1,1}$ and $R^{\pm}_{2,1}$ show that transport of the modulus of E and of its orientation are in some sense decoupled. This will help us to construct Riemann solvers.

Remark. Before building solvers we remark that in our framework, there is a natural (i.e., physical) notion of entropy. Here, the mathematical Lax entropy (see [8]) is the Hamiltonian $\mathcal{H}(D, B)$ and the flux of entropy is the Poynting vector $E \wedge B$. There is no viscosity principle that tells that this entropy should decrease. Nonetheless, this Kerr model neglects absorbtion in the medium (it also neglects dispersion, in fact). So the physics imposes that the entropy should not increase.

2.3. The 1-D Riemann Problem

Before going to numerical schemes, we have to study the 1-D Riemann problem which will help to design solvers. We first remark that the 1-D problem looks like a "p-system," so there is no result of existence or uniqueness of an entropic solution in general. In the case of one polarisation (i.e., $E_y = 0$ or $E_z = 0$) a result of Diperna states the global existence of a "viscosity solution" (cf. [3]). Under the same restriction we can use results of T.-P. Liu (cf. [10, 11]), who extends the condition of entropy, to ensure uniqueness in a certain class of entropic solutions. Nonetheless, there is no proof that the viscosity solution satisfies the extendable entropy conditon. Furthermore, T.-P. Liu's solution is not easily extensible to the system with the two polarisations. In this section we will show that, under the condition (L) that the speed of a 2-shock is smaller than the 1-speed, there is existence and uniqueness of the solution of the Riemann problem (one can refer to [15] for this condition). First we will exhibit the waves associated with the system.

2.3.1. *Contact Discontinuities*

The waves associated with $\lambda^{\pm}_1$ are contact discontinuities, and the modulus of the field E is unchanged through the discontinuity. We denote by E_{R}, B_{R} the right fields and E_{L}, B_{L}

the left ones. We have that $|E_R| = |E_L| = |E|$ and $E_R = |E|\sigma_R$, $E_L = |E|\sigma_L$. The Rankine–Hugoniot relationship implies that

$$B_R - B_L = \pm\sqrt{\mathcal{E}'\left(\frac{|E|^2}{2}\right)}(E_R - E_L) = \pm\sqrt{\mathcal{E}'\left(\frac{|E|^2}{2}\right)}|E|(\sigma_R - \sigma_L).$$

We remark that we could also have used the 1-Riemann invariants.

2.3.2. *2-Rarefaction Waves*

The 2-rarefaction waves do not modify the modulus of the electric field since it is a 2-Riemann invariant. If we look to self-similar fields $E = E(\xi) = E(x/t)$, $B = B(\xi) = B(x/t)$, then one has

$$\xi(|E|) = \lambda_2^{\pm} = \frac{\pm 1}{\sqrt{\mathcal{E}' + \mathcal{E}''|E|^2}}.$$

Since $|\lambda_2^{\pm}|$ is a decreasing function of $|E|$, one has $|E_L| > |E_R|$ for the $+$ wave, and the opposite for the $-$ wave. Furthermore, we denote $\sigma = E_L/|E_L| = E_R/|E_R|$. Since the 2-Riemann invariants are invariant (by definition) through a 2-wave and from the definition of G above, we have

$$B_R - B_L = \pm(G(|E_R|) - G(|E_L|))\sigma.$$

2.3.3. *2-Shocks*

We denote by $[U] = U_L - U_R$ the jump of the quantity U through the shock, $\bar{U} = (U_L + U_R)/2$, and by s the speed of the shock. The Rankine–Hugoniot relationship is

$$\begin{aligned} s[D] - [B] &= 0 \\ s[B] - [E] &= 0. \end{aligned} \tag{31}$$

We deduce that

$$s^2[D] - [E] = 0.$$

We denote $E = |E|\sigma$. Thus, we have

$$s^2(\overline{\mathcal{E}'|E|}[\sigma] + [\mathcal{E}'|E|]\bar{\sigma}) - |\bar{E}|[\sigma] - [|E|]\bar{\sigma} = 0.$$

We investigate the following cases.

- If $[|E|] = 0$ and $[\sigma] = 0$, there is not any shock.
- If $[|E|] = 0$ and $[\sigma] \neq 0$, then

$$s^2\overline{\mathcal{E}'|E|}[\sigma] = |\bar{E}|[\sigma],$$

so

$$s^2 = \frac{1}{\mathcal{E}'} = \frac{1}{\mathcal{E}'}$$

since $\mathcal{E}$ depends only on the modulus of E. So we are in the case of the 1-contact discontinuity.

- If $[|E|] \neq 0$, then E_L and E_R are colinear. Indeed, if they are independent, the jump condition implies that $s^2\mathcal{E}'_R = s^2\mathcal{E}'_L = 1$, which by no means is possible since we supposed that $|E_R| \neq |E_L|$. Thus, denoting by σ the common direction of E_R and E_L, one has $E_R = \alpha_R\sigma$ and $E_L = \alpha_L\sigma$. Here, $\alpha_{L\,or\,R}$ may be negative, positive, or zero. We finally get that the speed of the 2-shock satisfies

$$s^2 = \frac{[\alpha]}{[\mathcal{E}'(\alpha^2/2)\alpha]}$$

and

$$B_R - B_L = \pm\sqrt{\frac{[\mathcal{E}'(\alpha^2/2)\alpha]}{[\alpha]}}(E_R - E_L).$$

We notice that, when $[\alpha]$ tends to zero, s tends to $\lambda_2^{\pm}$.

2.3.4. Entropy Condition

Here we use the entropy and flux of entropy defined above. We will see how the decreasing of the entropy restricts the set of admissible shocks. Since the entropy is the Hamiltonian, and the flux of entropy is the Poynting vector, through a shock, one has

$$s\left[\mathcal{E}'|E|^2 - \mathcal{E} + \frac{|B^2|}{2}\right] - [E \cdot B] \leq 0.$$

Thanks to Rankine–Hugoniot relationships, one obtains

$$s(\bar{D}[E] - [\mathcal{E}]) \leq 0.$$

Since D is equal to $\partial_E\mathcal{E}$ and $\mathcal{E}$ is super-quadratic, one obtains that the speed of an entropic shock satisfies

$$s[|E|^2] \leq 0.$$

In other words, the upwind value of $|E|^2$ is smaller than the downwind one:

- If $s > 0$, then $|E_L| \leq |E_R|$.
- If $s < 0$, then $|E_R| \leq |E_L|$.

We notice that this does not ensure uniqueness since we can go from E_R to $E_L = -E_R/2$, either directly through a rightgoing 2-shock or through the combination of a rightgoing 1-contact discontinuity from E_R to $-E_R$ and then a rightgoing 2-shock from $-E_R$ to $-E_R/2 = E_L$.

2.3.5. *Condition (L) of Smoller and Johnson*

We need another condition to enforce uniqueness. We will adapt the condition (L) of Smoller and Johnson (see [15, p. 176]) to our case. Since $|\lambda_2^{\pm}| \leq |\lambda_1^{\pm}|$, denoting by U^+ the

upwind value of U for a 2-shock and by U^- the downwind one, we impose that, for entropic shocks,

$$(\mathrm{L})\ |s| \le |\lambda_1^{\pm}(E^-)|.$$

As $|E^+| \le |E^-|$, (L) is equivalent to

$$|s| \le \max|\lambda_1^{\pm}(E_{\mathrm{R}})|, |\lambda_1^{\pm}(E_{\mathrm{L}})|.$$

This implies that

$$\mathcal{E}'(|\alpha^-|^2/2) \le \frac{[\mathcal{E}'(|\alpha|^2/2)\alpha]}{[\alpha]},$$

which is equivalent to

$$\frac{(\mathcal{E}'(|\alpha^-|^2/2) - \mathcal{E}'(|\alpha^+|^2/2))\alpha^+}{\alpha^- - \alpha^+} \ge 0.$$

Since $|\alpha^+| \le |\alpha^-|$, one also has $\mathcal{E}'(|\alpha^+|^2/2) \le \mathcal{E}'(|\alpha^-|^2/2)$ and condition (L) is equivalent to

$$\frac{1}{\frac{\alpha^-}{\alpha^+} - 1} \ge 0,$$

or

$$\frac{\alpha^-}{\alpha^+} \ge 1.$$

Since $|\alpha^-|/|\alpha^+| \ge 1$ for entropic shocks condition (L) is equivalent to α^+ and α^- having the same sign.

Finally, we will call admissible 2-shocks those which fulfill both the entropy condition and condition (L). We can see that they are those for which E^+ and E^- point in the same direction of the sphere S^2, with $|E^+| \le |E^-|$.

2.3.6. Existence and Uniqueness of the 1-D Riemann Problem

In this section, we will show that, under the entropy condition and condition (L), we have existence and uniqueness for the Riemann problem.

LEMMA 2.5. *The only combinations of waves which are admissible are, from left to right, left* 1*-contact discontinuity, left admissible* 2*-shock or left* 2*-rarefaction wave, right admissible* 2*-shock or right* 2*-rarefaction wave, right* 1*-contact discontinuity.*

Proof. First, we remark that condition (L) and the fact that $|\lambda_2^{\pm}| \le |\lambda_1^{\pm}|$ implies that the 1-discontinuities must be at the two extremities of the chain. Second, for an admissible shock, one has

$$|\lambda_2^{\pm}(E^-)| \le s \le |\lambda_2^{\pm}(E^+)|.$$

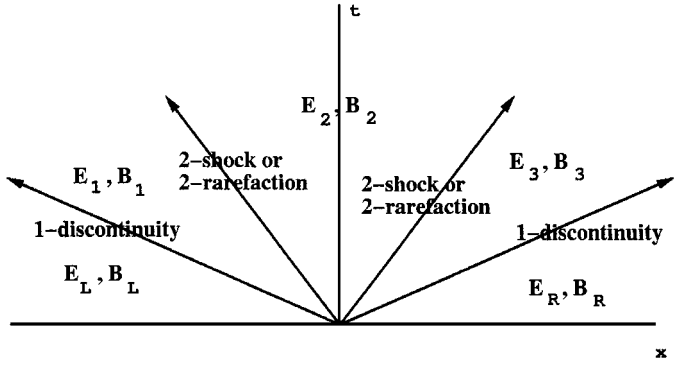

FIG. 1. Geometric situation of the Riemann problem.

Indeed, since $\mathcal{E}$ is super-quadratic, $\partial^2_{E,E}\mathcal{E}(E/|E|, E/|E|)$ is an increasing function of $|E|$ and so, thanks to Rolle's theorem, one has with $\sigma = E/|E|$

$$\frac{\partial^2\mathcal{E}(|E^+|^2)}{\partial E^2}(\sigma,\sigma) \le \frac{(\partial_E\mathcal{E}(|E^+|^2) - \partial_E\mathcal{E}(|E^-|^2))\cdot\sigma}{(E^+ - E^-)\cdot\sigma} \le \frac{\partial^2\mathcal{E}(|E^-|^2)}{\partial E^2}(\sigma,\sigma)$$

and so

$$\frac{1}{|\lambda_2^{\pm}(E^+)|^2} \le \frac{1}{s^2} \le \frac{1}{|\lambda_2^{\pm}(E^-)|^2}$$

The consequence of this inequality is that one cannot have a 2-shock and a 2-rarefaction wave in the same side. This ends the proof of the lemma. ■

Now, we are going to derive the existence and uniqueness of the Riemann problem. Thanks to the previous lemma, we are in the situation depicted in Fig. 1.

Let us call F the following function:

$$\begin{aligned}
&\mathbb{R}^+ \times \mathbb{R}^+ \mapsto \mathbb{R}\\
&F\colon (X,Y) \mapsto G(Y) - G(X) && \text{if } X > Y\\
&\qquad (X,Y) \mapsto \sqrt{\frac{\mathcal{E}'\left(\frac{Y^2}{2}\right)Y - \mathcal{E}'\left(\frac{X^2}{2}\right)X}{Y - X}}\cdot(Y - X) && \text{if } X < Y
\end{aligned}$$

We then express the conditions linking the different fields in Fig. 1 from left to right.

Left contact discontinuity: One has

$$|E_1| = |E_{\mathrm{L}}|, \qquad \sigma_1 = \frac{E_1}{|E_1|}, \qquad \sigma_{\mathrm{L}} = \frac{E_{\mathrm{L}}}{|E_{\mathrm{L}}|},$$

and

$$B_1 - B_{\mathrm{L}} = -\sqrt{\mathcal{E}'\left(\frac{|E_{\mathrm{L}}|^2}{2}\right)}|E_{\mathrm{L}}|(\sigma_1 - \sigma_{\mathrm{L}}).$$

Left 2-shock or 2-rarefaction wave: One has

$$\frac{E_2}{|E_2|} = \sigma_2 = \sigma_1 \qquad \text{and} \qquad B_2 - B_1 = \sigma_2 F(|E_2|, |E_{\mathrm{L}}|).$$

From this we deduce

$$B_2 - B_{\mathrm{L}} = \sqrt{\mathcal{E}'\left(\frac{|E_{\mathrm{L}}|^2}{2}\right)}E_{\mathrm{L}} - \sigma_2\left(\sqrt{\mathcal{E}'\left(\frac{|E_{\mathrm{L}}|^2}{2}\right)}|E_{\mathrm{L}}| - F(|E_2|, |E_{\mathrm{L}}|)\right). \quad (32)$$

Similarly, one has

Right 2-shock or 2-rarefaction wave: One has

$$\sigma_2 = \sigma_3 = \frac{E_3}{|E_3|} \qquad \text{and} \qquad B_3 - B_2 = \sigma_2 F(|E_2|, |E_3|).$$

Right contact discontinuity: One has

$$|E_3| = |E_{\mathrm{R}}|, \qquad \sigma_{\mathrm{R}} = \frac{E_{\mathrm{R}}}{|E_{\mathrm{R}}|}, \qquad \text{and} \qquad B_{\mathrm{R}} - B_3 = \sqrt{\mathcal{E}'\left(\frac{|E_{\mathrm{R}}|^2}{2}\right)}|E_{\mathrm{R}}|(\sigma_{\mathrm{R}} - \sigma_2).$$

From this we deduce

$$B_{\mathrm{R}} - B_2 = \sqrt{\mathcal{E}'\left(\frac{|E_{\mathrm{R}}|^2}{2}\right)}E_{\mathrm{R}} - \sigma_2\left(\sqrt{\mathcal{E}'\left(\frac{|E_{\mathrm{R}}|^2}{2}\right)}|E_{\mathrm{R}}| - F(|E_2|, |E_{\mathrm{R}}|)\right). \quad (33)$$

Summing Eqs. (32) and (33), we obtain

$$\begin{aligned} &B_{\mathrm{R}} - B_{\mathrm{L}} - \left(\sqrt{\mathcal{E}'\left(\frac{|E_{\mathrm{R}}|^2}{2}\right)}E_{\mathrm{R}} + \sqrt{\mathcal{E}'\left(\frac{|E_{\mathrm{L}}|^2}{2}\right)}E_{\mathrm{L}}\right) \\ &= \sigma_2(F(|E_2|, |E_{\mathrm{R}}|) + F(|E_2|, |E_{\mathrm{L}}|)) - \sigma_2\left(\sqrt{\mathcal{E}'\left(\frac{|E_{\mathrm{R}}|^2}{2}\right)}|E_{\mathrm{R}}| - \sqrt{\mathcal{E}'\left(\frac{|E_{\mathrm{L}}|^2}{2}\right)}|E_{\mathrm{L}}|\right), \end{aligned} \quad (34)$$

which is an equation in E_2. Thus the existence and uniqueness of the solution of the Riemann problem amount to the existence and uniqueness of E_2 solution of the previous equation.

LEMMA 2.6. *In expression* (34), *the factor of* σ_2 *is a continuous, decreasing function of* $|E_2|$, *going from* 0 *to* $-\infty$, *when* $|E_2|$ *goes from* 0 *to* $+\infty$.

Proof. Indeed, first, if $|E_2| = 0$, it is clear that the factor vanishes. Second, since $F(X, Y)$ is continuous, the factor is continuous. In fact, F is C^1. Third, when $X < Y$,

$$\partial_X F(X, Y) = \frac{\mathcal{E}'\left(\frac{X^2}{2}\right)X - \mathcal{E}'\left(\frac{Y^2}{2}\right)Y + (X - Y)\left(\mathcal{E}'\left(\frac{X^2}{2}\right) + X^2 \cdot \mathcal{E}''\left(\frac{X^2}{2}\right)\right)}{2\sqrt{F(X, Y)}} < 0$$

since $X < Y$. When $X > Y$,

$$\partial_X F(X,Y) = -\sqrt{\mathcal{E}'\left(\frac{X^2}{2}\right) + X^2 \cdot \mathcal{E}''\left(\frac{X^2}{2}\right)} < 0.$$

Furthermore, Since $\mathcal{E}$ is strictly convex in E,

$$\sqrt{\mathcal{E}'\left(\frac{X^2}{2}\right) + X^2 \cdot \mathcal{E}''\left(\frac{X^2}{2}\right)}$$

is bounded from below and so $F(X,Y)$ goes to $-\infty$ when X goes to $+\infty$. This ends the proof of the lemma. ■

Now, if the left-hand side of Eq. (34) is vanishing, then $|E_2| = 0$ and σ_2 is not determined but $E_2 = 0$ is the unique solution.

If the left-hand side does not vanish, it can be written as $|\mathrm{LHS}|\sigma_{\mathrm{LHS}}$ with obvious notations. Thus $\sigma_2 = -\sigma_{\mathrm{LHS}}$ and $|E_2|$ is uniquely determined thanks to the previous lemma.

Finally, if E_2 does not vanish, we can go back to E_1 and E_3 in a unique way, and so for the magnetic fields.

If $E_2 = 0$, the 1-discontinuities and the 2-shocks have the same slope and so there is is no room for E_3 and E_1. Once again we go back to B_2 in a unique way.

So finally we have obtained.

THEOREM 2.1. *The system* (16) *with* $(E(t=0),\ B(t=0)) = (E_{\mathrm{L}},\ B_{\mathrm{L}})$ *if* $x < 0$ *and* $(E(t=0),\ B(t=0)) = (E_{\mathrm{R}},\ B_{\mathrm{R}})$ *when* $x > 0$ *has a unique solution compounded of contact discontinuities, shocks, and rarefaction waves under the condition of diminishing entropy and condition* (L).

Before going into numerical issues we add a physical comment. The previous results have shown a kind of decoupling between the phase and the modulus of the electric field, each being tied to a different Riemann invariant and thus propagating at a different speed.

3. THE DISCRETIZATION SCHEME

In this section we begin by recalling the basics about finite volume techniques (see also [9]). Then we will describe more precisely two types of fluxes and two time schemes.

3.1. Finite Volume Space Discretisation

We denote by Ω_h the approximate domain of computation, by $\mathcal{T}_h$ a tesselation of Ω_h, and by W_h the approximation of W on $\mathcal{T}_h$. We also denote by C_i the cells of $\mathcal{T}_h$, by ∂C_i their boundaries, and by ∂C_{ij}, the set $\partial C_i \cap \partial C_j$. W_i is the approximate value of W in the cell ∂C_i. If we denote symbolically our hyperbolic system

$$\partial_t W + \mathrm{div}\, F(W) = 0, \tag{35}$$

then, integrating in each cell C_i, we obtain

$$\partial_t \int_{C_i} W\,dx + \sum_j \int_{\partial C_{ij}} F(W)n\,d\sigma = 0, \tag{36}$$

where n is the outgoing normal. Now the first term is replaced by $W_i|C_i|$, where $|C_i|$ is the volume of C_i. Most of the solvers' technology relies on the choice of the value of W used in the second integral. This integral is replaced by

$$\sum_j \int_{\partial C_{ij}} \Phi_{ij},$$

where Φ_{ij} is the flux function associated to a particular scheme.

3.1.1. Godunov Fluxes

In the case of a Godunov scheme,

$$\Phi_{ij} = \Phi_{ij}^G = n \cdot F(W^G(W_i, W_j)),$$

where $W^G(W_i, W_j)$ is the exact solution on $x = 0$ of the 1-D Riemann problem with the following Cauchy data:

$$\text{for } x \le 0; \quad W = W_i \qquad \text{and} \qquad \text{for } x > 0; \quad W = W_j.$$

In general, these fluxes are not easy to compute since one has to know exactly the function G of the previous section.

3.1.2. Roe Fluxes

In the case of Roe fluxes, we solve the Riemann problem, but instead of using entropic and (L) conditions, we enforce to have only shocks. So, if we define the matrix $A^{\mathrm{R}}(W_i, W_j)$ to be such that $F(W_i) - F(W_j) = A^{\mathrm{R}}(W_i, W_j)(W_i - W_j)$, then we define W^{R} as the solution in $x = 0$ of

$$\partial_t W + A^{\mathrm{R}}(W_i, W_j)\,\partial_x W = 0$$

with the same Cauchy data as for the Godunov fluxes. Finally the Roe flux is

$$\Phi_{ij} = \Phi_{ij}^{\mathrm{R}} = n \cdot F(W^{\mathrm{R}}(W_i, W_j)).$$

It can also be shown that

$$\Phi_{ij}^{\mathrm{R}} = n \cdot \left(\frac{F(W_i) + F(W_j)}{2} - |A(W_i, W_j)|(W_j - W_i) \right).$$

This way is more easy to implement since one only has to compute the matrix A. Nonetheless, it leads to nonadmissible shocks. But we will see that for small discontinuities, the results resemble those obtained with Godunov fluxes.

3.1.3. High-Order Approximations

As is well known, the two methods presented above are only approximations of order 1 in space. We will use the idea of the MUSCL technique developed by Van Leer (see [6, 18]). The idea is to change the right and left values in the flux functions according to an interpolation scheme. Namely, we use W_{ij} and W_{ji}, where the first one is a third-order approximation on the i side of the interface and the second one is a third-order approximation on the j side. In one dimension, on a regular mesh, it amounts to

$$W_{i\,i+1} = (5/6)W_i + (2/6)W_{i+1} - (1/6)W_{i-1},$$

and

$$W_{i+1\,i} = (5/6)W_{i+1} + (2/6)W_i - (1/6)W_{i+2}.$$

This leads to third-order spatial approximations in the case of regular meshes.

3.2. Time Discretisation

To increase the time order we have used the order 2 Hancock predictor corrector scheme (see [19]) and an order 3 nonlinear Runge–Kutta scheme (see for instance [12] for a discussion on this time scheme).

4. NUMERICAL RESULTS

In this section, we set $\mathcal{E}(|E|^2/2) = E^2/2 + E^4/12$ so that $D = E(1 + |E|^2/3)$ and

$$G(|E|) = \frac{\log(|E| + \sqrt{1+|E|^2}) + |E|\sqrt{1+|E|^2}}{2}.$$

4.1. 1-D Results

The first experiments are done on an infinite line (i.e., we have implemented periodic boundary conditions). The space step is set to 0.001. In the first series, we compare Godunov scheme, Godunov scheme + predictor–corrector and order 2 MUSCL technique, and the same with an order 3 MUSCL technique. The first test is with a rightgoing wave satisfying at $t = 0$ if $x < 0.25$ or $x > 0.75$, then $E = 0$, else $E_z = 1$. For order 1 and order 3, the time step is set to 0.001. For reasons of stability, it is set to 0.0005 for order 2. Results at $t = 1$ are presented in Fig. 2. The first remark is that the shock speed is well predicted by the three approximations. The second one is that order 1 seems to be the best, but this is due to the special choice for the time step. This cannot be reproduced in multi dimensional simulations. The third remark is that order 2 is more unstable than the others, and the last remark is that both order 2 and order 3 produce spurious oscillations around the shock. This is a well-known fact.

Now, we change the initial situation. We use if $x < 0.25$ or $x > 0.75$, then $E = 0$, else $E_z = 0.2 + 0.8 * \mathrm{sign}(x - 0.5)$. Results are plotted in Fig. 3. In this case, the results are very different. The first order completely misses the good solution of the Riemann problem with condition (L). In fact, it could be shown that it converges toward the solution of the Riemann

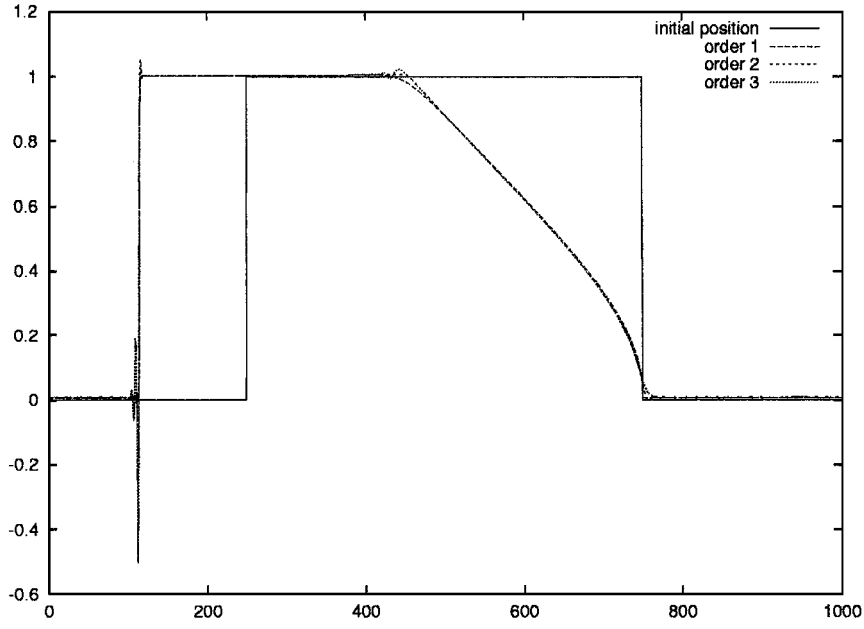

FIG. 2. Squared wave for Godunov's solver-I.

problem with the T.-P. Liu condition. Order 2 is not precise on the capture of the contact discontinuity, since this one should be between 1 and -1, so here, the error is of 20%. We again observe the oscillations at the back of the shocks.

The next case is almost the same but we permute the upwind and downwind initial values, so that the contact discontinuity is followed by a rarefaction wave. So we use if $x < 0.25$

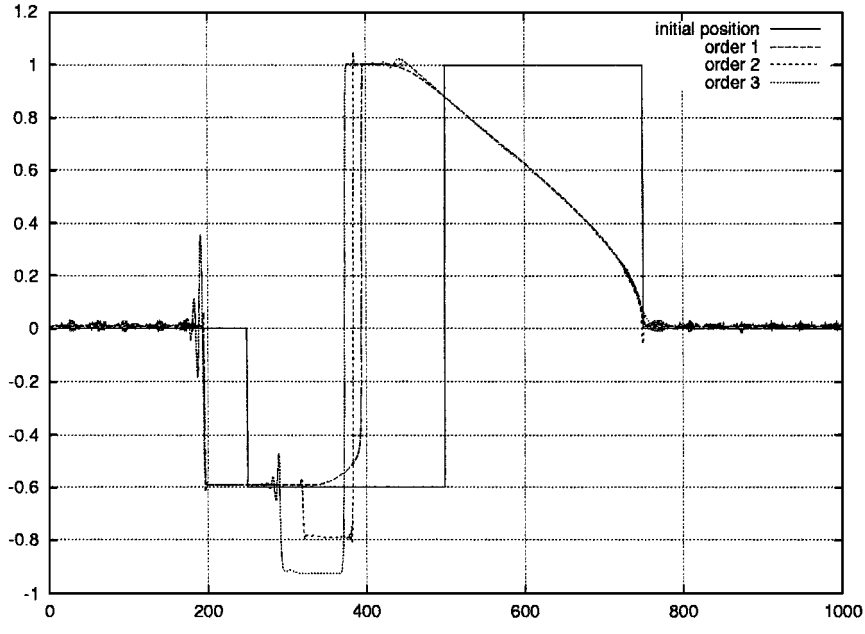

FIG. 3. Local Riemann problem for Godunov's solver.

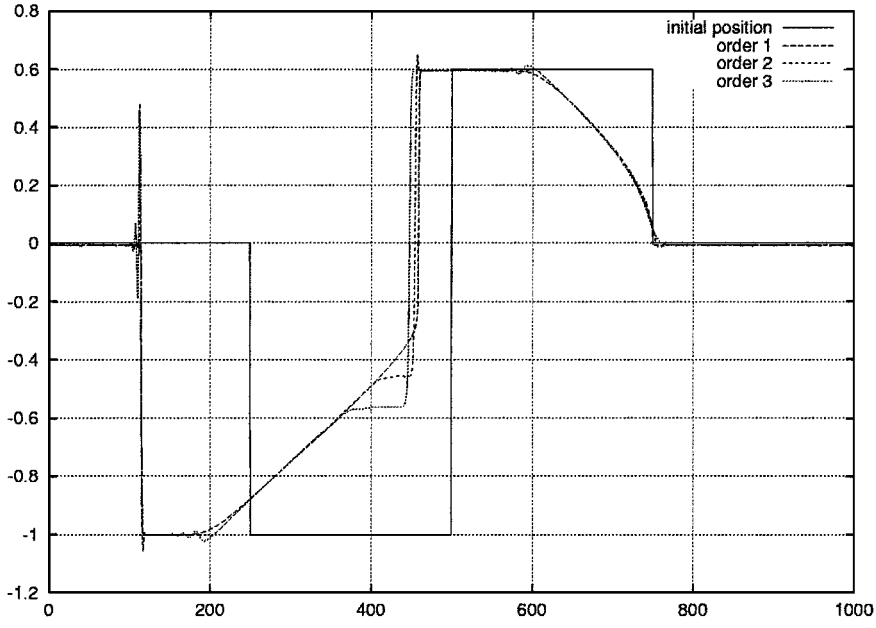

FIG. 4. Local Riemann problem for Godunov's solver-II.

or $x > 0.75$, then $E = 0$, else $E_z = -0.2 + 0.8 * \text{sign}(x - 0.5)$. The results are presented in Fig. 4. Here again, we observe that order 1 misses the good solution and that order 3 is better than order 2 except for the oscillations at the back of the shocks.

The last case of this series is the consideration of a wave packet:

$$E_z = e^{-100*(x-0.5)^2} * \cos((x - 0.5) * \pi * 40).$$

This case is of importance, since Kerr–Maxwell models are mainly used to simulate high-frequency beams or solitary structures. The results are shown in Fig. 5. Here, we can see the diffusive effect of the order 1 scheme. Furthermore, we can observe that the dephasing is much more emphasised with the third-order approximation. This effect is in accordance with the physics. Indeed, since the index of the medium increases with the value of the electric energy, the wavelength diminishes. This is what we observe at the back of the wave packet.

In the next series of results we compare the Roe solver with the Godunov solver, both with either predictor–corrector or order 3 Runge–Kutta scheme. The spatial approximation will be the order 3 one. The first test corresponds to the second one of the previous series. At $t = 0$, we use if $x < 0.25$ or $x > 0.75$, then $E = 0$, else $E_z = 0.2 + 0.8 * \text{sign}(x - 0.5)$. Results are shown in Fig. 6. Here we remark that Roe and Godunov coincide perfectly, so that we mainly compare here the time schemes. Thus, the second remark is that the predictor–corrector is more accurate for the speeds and levels of the shocks but also more oscillatory.

The next test corresponds to the third of the previous series: At $t = 0$, we use if $x < 0.25$ or $x > 0.75$, then $E = 0$, else $E_z = -0.2 + 0.8 * \text{sign}(x - 0.5)$. Results are shown in Fig. 7. Again we remark that Roe and Godunov coincide and that the predictor–corrector is more accurate and more oscillatory than the Runge–Kutta scheme.

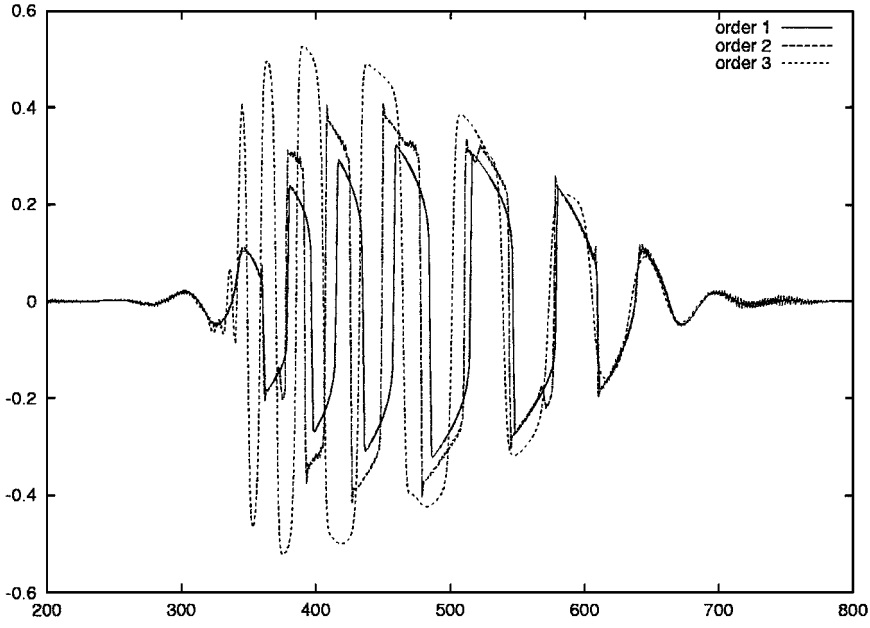

FIG. 5. Wave packet for Godunov's solver.

The last 1-D test is about the wave packet. At $t = 0$,

$$E_z = e^{-100*(x-0.5)^2} * \cos((x - 0.5) * \pi * 40),$$

and the results are shown in Fig. 8. We observe again the perfect accordance of Roe and

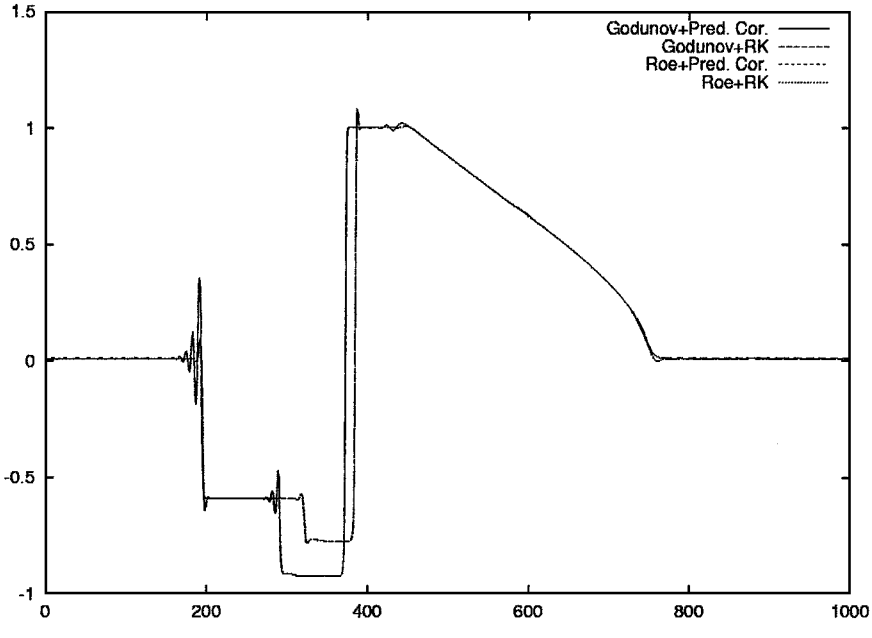

FIG. 6. Comparison of Roe and Godunov with Runge–Kutta or predictor–corrector.

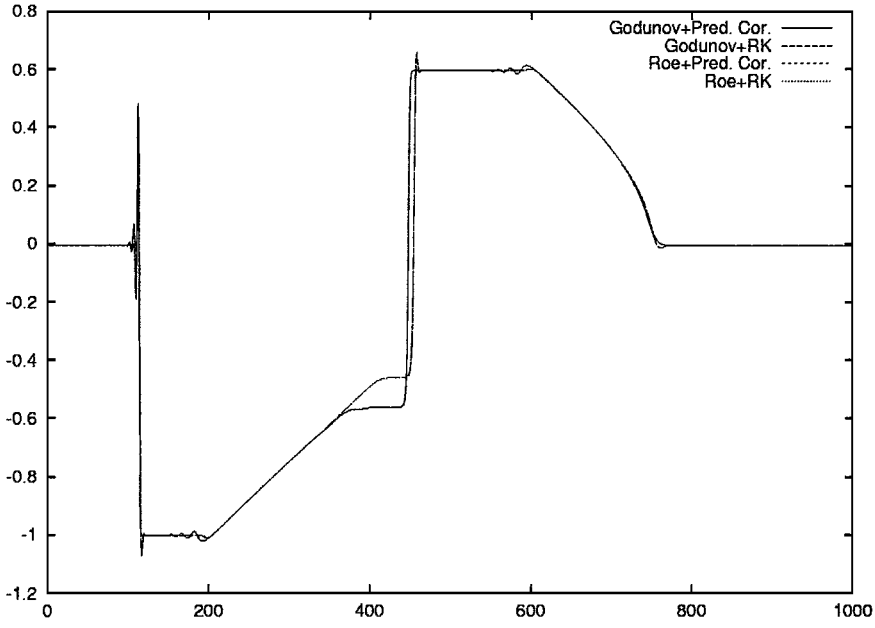

FIG. 7. Comparison of Roe and Godunov with Runge–Kutta or predictor–corrector.

Godunov solvers. The better quality of the predictor–corrector is demonstrated here by the fact that it is less diffusive and better reflects the variation of the wavelength than the Runge–Kutta scheme. For this reason we now make the choice of using only the predictor–corrector. Furthermore, since the Roe solver is much cheaper than the Godunov one and since they coincide, we make the choice of using the first one.

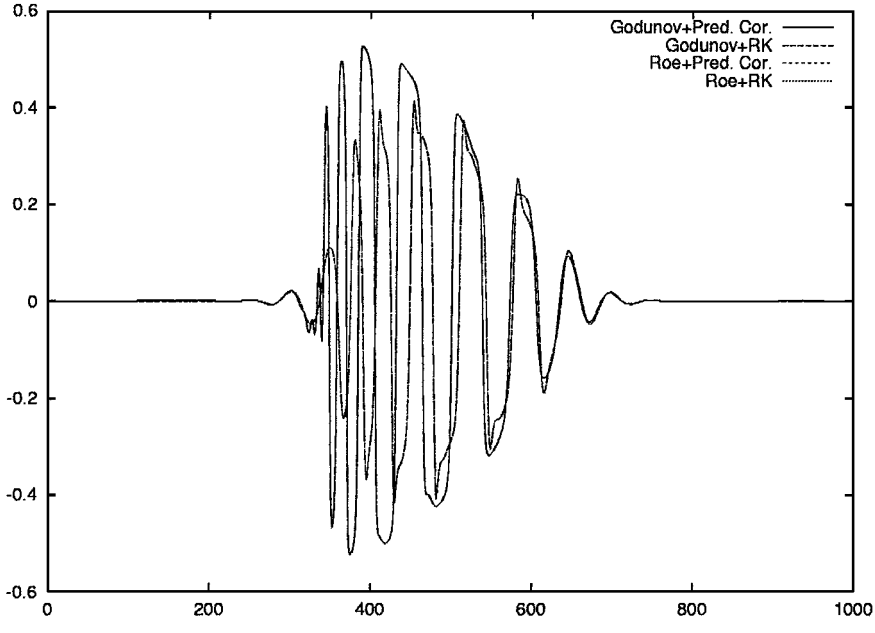

FIG. 8. Comparison of Roe and Godunov with Runge–Kutta or predictor–corrector.

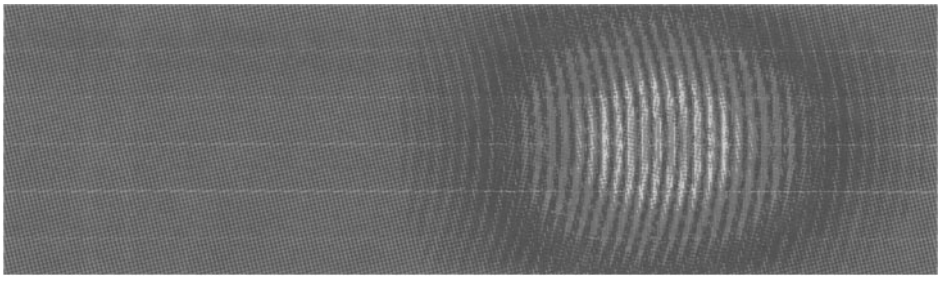

FIG. 9. A wave packet in a linear medium.

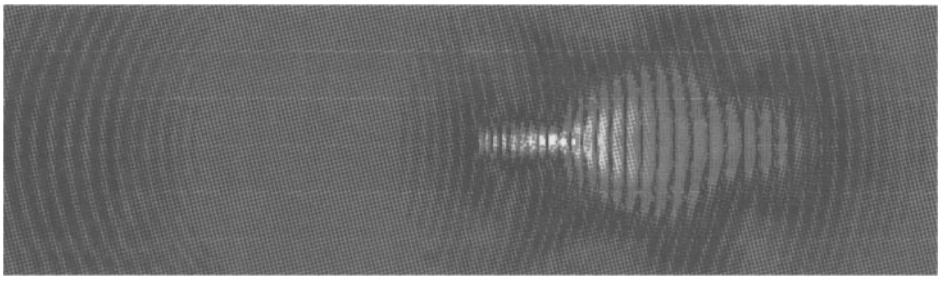

FIG. 10. A wave packet in a nonlinear medium.

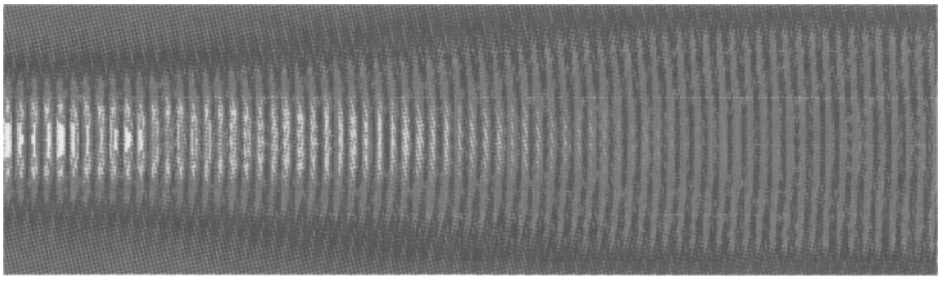

FIG. 11. A Gaussian beam in a linear medium.

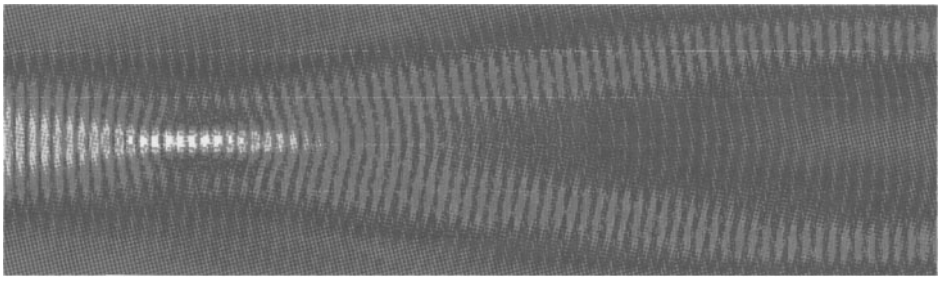

FIG. 12. A Gaussian beam in a nonlinear medium ($W_0 = 2^* \lambda$).

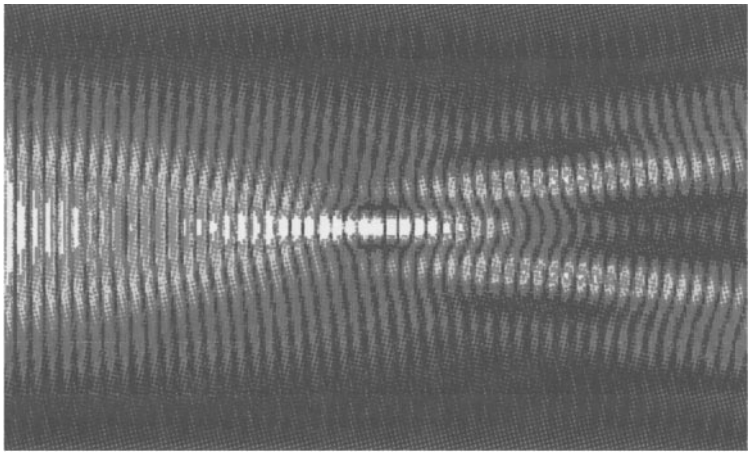

FIG. 13. A Gaussian beam in a nonlinear medium ($W_0 = 4^* \lambda$).

4.2. 2-D Results

In this section, we present two test cases. The first one is a wave packet through either a linear medium or a nonlinear one. The second case is a Gaussian beam travelling through the same types of media. The domain of computation is the rectangle $[0; 0.7] \times [0; 0.2]$. The spatial step of discretisation is $\Delta x = \Delta y = 10^{-3}$ and the time step is $\Delta t = 0.5 \times 10^{-3}$. We begin by a wave packet propagating rightward. At $t = 0$ we set

$$E_z = 2e^{-100*(x-0.25)^2} e^{-2500*(y-0.1)^2} * \cos(100\pi(x - 0.5)),$$

and we present the modulus of the electric field at $t = 250$. In the linear medium (Fig. 9), we observe that the packet spreads itself and that its maximum intensity diminishes. In the nonlinear medium (Fig. 10), the packet is concentrated along its axis and its maximum intensity is greater than the initial one. This is a typical behavior of a Kerr medium.

For the Gaussian beam, we use as an ingoing boundary condition at $x = 0$ an electric field polarized along the z axis. The wavelength is $\lambda = 1/50$, and the belt radius is chosen as $w_0 = 2 * \lambda$, so that the angle of aperture of the beam is $\theta = \arctan(\lambda/(\pi w_0)) = 9^\circ$,

$$E_z(x = 0) = e^{-y^2/w_0^2} \sin(\omega t),$$

with $\omega = 2\pi/\lambda$. For details about Gaussian beams, one can refer, for instance, to [2]. We observe the beam at $t = 1000$. In Fig. 11 the beam propagates approximately with the angle of aperture θ. To the contrary, in the Kerr medium we can see (Fig. 12) that the beam first concentrates (it is the self-focusing effect) and then splits into two filaments as it is classically observed in the experiments. In the last picture (Fig. 13), we have doubled the value of w_0 and thus the energy of the 2D beam. The nonlinear medium is unchanged. Nonetheless, we have modified the size of the computation box to improve the comprehension of the picture. The box is now $[0; 0.5] \times [0; 0.3]$. We observe here that the number of filaments is increased.

5. CONCLUDING REMARKS

This paper presents the derivation of a numerical scheme for the propagation of electromagnetic waves in Kerr nonlinear media. We first noted the hyperbolicity of the system.

Then we obtained existence and uniqueness for the Riemann problem for large data. We used this result to build a Godunov scheme. We observed that the Roe solver led to the same results as the Godunov one. Finally we demonstrated the efficiency of our method on the simulation of a multi-filamentation of a Gaussian beam.

REFERENCES

1. N. Bloembergen, *Nonlinear Optics* (Benjamin, Elmsford, NY, 1965).
2. D. Dangoisse, D. Hennequin, and V. Zehné-Dhaoui, *Les lasers* (Dunod, Paris, 1998).
3. R. J. Diperna, Convergence of approximate solutions to conservation laws, *Arch. Rational Mech. Anal.* **82**, 27 (1983).
4. P. Donat, *Quelques contributions mathématiques en optique non linéaire*, thèse de doctorat, Ecole polytechnique, 1994.
5. P. Donat and J. Rauch, Global solvability of the Maxwell–Bloch equations for nonlinear optics, *Arch. Rational Mech. Anal.* **136**, 291 (1996).
6. L. Fezoui and B. Stoufflet, A class of implicit upwind schemes for euler simulations with unstructured meshes, *J. Comput. Phys.* **84**, 174 (1989).
7. G. Grynberg, A. Aspect, and C. Fabre, *Introduction aux lasers et à l'optique quantique* (Ellipses, 1997).
8. P. D. Lax, *Hyperbolic Systems of Conservation Laws and the Mathematical Theory of Shocks Waves* (Soc. for Industr. & Appl. Math., Philadelphia, 1973).
9. P. D. Lax, A. Harten, and B. Van Leer, On upstream differencing and Godunov type schemes for hyperbolic conservation laws, *SIAM Rev.* **25** (1983).
10. T.-P. Liu, The Riemann problem for general 2×2 conservation laws, *Trans. Amer. Math. Soc.* **199**, 99 (1974).
11. T.-P. Liu, Existence and uniqueness theorems for Riemann problems, *Trans. Amer. Math. Soc.* **212**, 375 (1975).
12. S. Piperno and S. Depeyre, Criteria for the design of limiters yielding efficient high resolution tvd schemes, *Comput. & Fluids* **27**, 183 (1998).
13. R. Racke, *Lectures on Nonlinear Evolution Equations* (Vieweg, Wiesbaden, 1992).
14. L. Schwartz, *Analyse hilbertienne, Collection Méthodes* (Hermann, Paris, 1979).
15. J. A. Smoller and J. L. Johnson, Global solutions for an extended class of hyperbolic systems of conservation laws, *Arch. Rational Mech. Anal.* **32**, 169 (1969).
16. A. Taflove, *Computational Electrodynamics, the Finite-Difference Time-domain Method* (Artech House, Norwood, MA, 1995).
17. M. E. Taylor, *Pseudodifferential Operators* (Princeton Univ. Press, Princeton, 1981).
18. B. Van Leer, Towards the ultimate conservative difference schemes. V: A second order sequel to Godunov's method, *J. Comput. Phys.* **32** (1979).
19. B. Van Leer, *On the Relation between the Upwind-Differencing Schemes of Godunov, Engquist-Osher and Roe*, Tech. Report 81-11, ICASE, Mar. 1981.